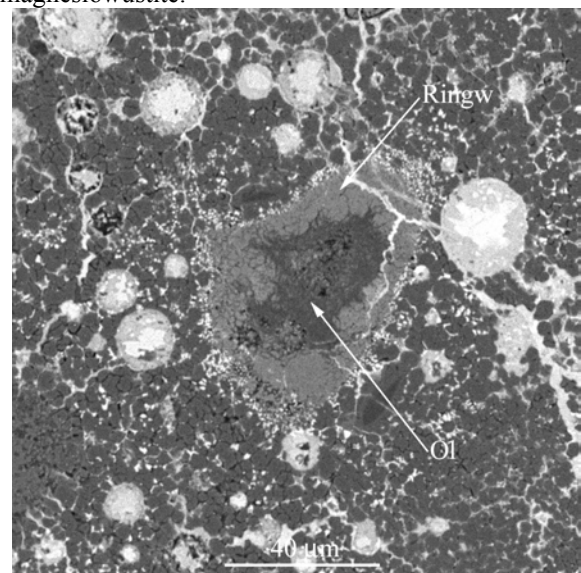


**RINGWOODITE-OLIVINE ASSEMBLAGES IN DHOFAR 922 L6 MELT VEINS.** D. D. Badjukov<sup>1</sup>, F. Brandstaetter<sup>2</sup>, G. Kurat<sup>3</sup>, E. Libowitzky<sup>3</sup> and J. Raitala<sup>4</sup>, <sup>1</sup>V.I. Vernadsky Institute RAS, Kosygin str. 19, 11991, Moscow, Russia, [badyukov@geokhi.ru](mailto:badyukov@geokhi.ru), <sup>2</sup>Naturhistorisches Museum, Burgring 7, A-1010 Wien, Austria, [franz.brandstaetter@nhm-wien.ac.at](mailto:franz.brandstaetter@nhm-wien.ac.at), <sup>3</sup>Universität Wien, Institut für Geologische Wissenschaften, Althanstr. 14, A-1090 Wien, Austria, [gero.kurat@univie.ac.at](mailto:gero.kurat@univie.ac.at), <sup>4</sup>University of Oulu, FIN 90401, Finland, [jouko.raitala@oulu.fi](mailto:jouko.raitala@oulu.fi),

**Introduction.** Shock-induced melt veins stand out among different types of veins in ordinary chondrites due to their specific mineral assemblages. They often contain high pressure polymorphs of host chondrite minerals like wadsleyite, ringwoodite, majorite, akimotoite and so on [1-4]. Because of a compositional similarity between chondrites and the Earth's mantle, the shock melt veins are an unique natural source of study of mantle mineralogy. Two lithologies are characteristic for the veins: silicates, oxide(s), sulfide(s) and metal crystallized from a melt and solid state re-crystallized minerals of the vein hosts. All but a few the shock veins containing high-pressure phases have been found in L6 chondrites. Using data on desert meteorites [5] one can count the amount of L6 chondrites containing ringwoodite to be ~1.5 % of all L6 finds. The estimate gives a minimum value because thin sections used for meteorite descriptions do not always include such veins, even if they are present in the rock. Vein textures and mineralogy require a compressional molten state of vein matter. Different mechanisms have been proposed for the high temperature excursions during a shock pulse: adiabatic shear zones, collisions of incident shock wave fronts and collapses of open spaces [6]. Here we report on the mineralogy of shock melt veins containing HP phases in the Dhofar 922 L6 chondrite. The aim of the work is to establish the temperature-pressure history of the veins.

**Observations.** Optical microscopy, Raman spectroscopy, analytical SEM, and an EMP were used for identification and chemical characterization of phases. Dhofar 922 has the usual chondritic mineralogy: olivine (Fa<sub>23.1</sub>), low-Ca pyroxene (Fs<sub>20.2</sub>Wo<sub>2.8</sub>), Ca-pyroxene (Fs<sub>8.4</sub>Wo<sub>44.0</sub>), maskelynite, chromite and apatite. Metal in the outer part of the meteorite is oxidized due to terrestrial weathering. Melt veins form an irregular net, which divides the host chondrite into cm-sized clasts. The vein thickness ranges from 3 μm to 1.5 mm. The veins consist of a matrix that contains numerous clasts. The matrix is composed of a few μm-sized euhedral crystals of majorite - garnet solid solution with 0.4 wt% Na<sub>2</sub>O, minor (Mg,Fe)<sub>2</sub>SiO<sub>4</sub> phase (ringwoodite?), interstitial magnesiowüstite and troilite and somewhat oxidized metal spheres. The matrix at vein margins has a quench texture: (Mg,Fe)SiO<sub>3</sub> and (Mg,Fe)<sub>2</sub>SiO<sub>4</sub> phases form dendritic and fork-like crystals embedded in glass. Broad-beam EMP analyses of vein matrix

gave in average a composition enriched in Al and Ca relatively to the host chondrite, which is proposed to be due to preferred melting of plagioclase. Embedded in the veins are non-melted inclusions of the host chondrite which were converted to different phases, common are ringwoodite, olivine, majorite, pyroxene and plagioclase glass. Several areas contain also green wadsleyite aggregates. Some majorite and ringwoodite clasts are enveloped by a silica mantle. Ringwoodite is observed also at a distance of no more than ~0.5 mm from vein walls in the host rock. Usually, the high-pressure phases have the same chemical compositions as olivine and pyroxenes of the chondrite, although there are exceptions. Part of former olivine clasts were converted to ringwoodite-olivine assemblages that consist of olivine cores and ringwoodite rims (Fig. 1). The compositions of the phases are more or less the same. The olivine has a lower Fe content (Fa<sub>9.5±1.1</sub>) than the ringwoodite (Fa<sub>40.5±2.7</sub>). Occasionally, it seems that the ringwoodite rims are composed of tiny crystals although in most cases the structure of the rims is irresolvable using optical and SEM techniques. Outer margins of the ringwoodite rims contain tiny grains of magnesiowüstite.



**Fig.1.** SEM image of olivine-ringwoodite inclusion embedded in majorite - magnesiowüstite matrix. Magnesiowüstite is present also around the inclusion (tiny light gray dots).

**Discussion.** Morphology and structure of the olivine-ringwoodite inclusions suggest that the olivine clasts experienced solid-state high pressure

transformation without melting and the transformation was accompanied by diffusion of Fe. Compositions of co-existing olivine and ringwoodite correspond to 1200 °C and 12.7 GPa according to the  $Mg_2SiO_4 - Fe_2SiO_4$  diagram (Fig. 2). The estimation is supported by the presence of wadsleyite accumulations in some vein areas because the tie line is very close to the stability field of wadsleyite. The agreement of the olivine and ringwoodite compositions with thermodynamically calculated compositions of the phases [7,8] implies a close to equilibrium state in the clasts. On the other hand, magnesiowustite in the veins can be considered as a product of ringwoodite decomposition to stishovite and magnesiowustite or to perovskite and magnesiowustite. The reactions occur at pressures up to 23 - 25 GPa. In addition, preliminary data on olivine and pyroxene X-ray diffraction peak broadening in the host rock and the presence of rare birefringent plagioclase in maskelynite give an estimation of a peak shock pressure to be 28 - 35 GPa.

Based on this, we propose a model for the vein shock history: A shock wave was generated by collision of an L chondrite parent asteroid with another body. When a shock wave came to a source area of L6 chondrites, the pressure pulse had obtained a curvilinear triangular shape due to its attenuation and the duration of the high pressure regime was much shorter compared with a duration of a compression at lower pressure. Crystallization of majorite from melt and decomposition of  $(Mg,Fe)_2SiO_4$  occurred at the high pressure regime at 30 - 22 GPa, whereas formation of wadsleyite and olivine-ringwoodite assemblages took place at lower pressure.

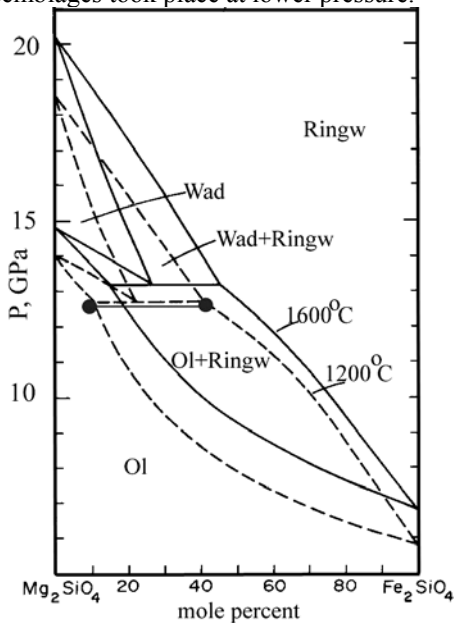


**Fig. 2.** The  $Mg_2SiO_4$ - $Fe_2SiO_4$  diagram [7]. Black dots denote average compositions of co-existing olivine and ringwoodite.

The melt veins were formed at the shock wave front, probably due to adiabatic shear because temperatures necessary for melting can not be reached by a collision of incident shock wave fronts as calculations of shock temperatures for L chondrites demonstrate (Fig. 3). In a perpendicular collision of plane shock waves the shock pressure is doubled and the resulting shock temperature can not be increased more than twice and, hence, by 35 GPa the shock collision temperature can not be more than 980 °C. The duration of cooling the hot zones to 1200 °C can be estimated by a numerical solution of the heat flow equation which gives approximately 2 sec for a 1 mm thick melt vein. This seems to be sufficient for establishing an equilibrium between olivine and ringwoodite.

**Acknowledgments.** This study was supported by Austrian Academy of Sciences, the Austria-Russia project RFBR - BSTC (project Nr 14/04) and the Academy of Finland.

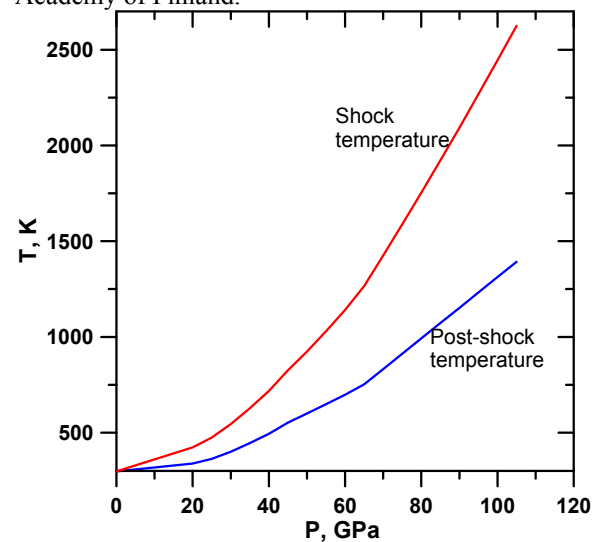


**Fig. 3.** Calculated post-shock and shock temperatures for L chondrites.

**References:** [1] R. A. Binns et al., *Nature*, 221, 943 (1969) [2] Smith J.V., Mason B., *Science*, 168, 832 (1970) [3] T. G. Sharp et al., *Science* 277, 352 (1997). [4] Langenhorst F., Porier J.P., *EPSL*, 184, 37, (2000) [5] Meteoritical Bulletin, NN 83 - 88, *Meteoritics & Planetary Science* 34, A169 (1999), 35, A199 (2000), 36, A293 (2001), 37, A157 (2002), 38, A189 (2003), 39, (2004). [6] J. G. Spray, *Geology* 27, 695 (1999). [7] D. C. Presnall. Phase diagrams of Earth-forming minerals. In: *Mineral Physics and Crystallography*, AGU Reference Shelf 2, 248, (1995). [8] Y. Fey et al., *JGR* 96, 2157 (1991)